

*promoting access to White Rose research papers*



**Universities of Leeds, Sheffield and York**  
**<http://eprints.whiterose.ac.uk/>**

---

This is the Author's Accepted version of an article published in the **Journal of Non-Newtonian Fluid Mechanics, 205**

White Rose Research Online URL for this paper:

<http://eprints.whiterose.ac.uk/id/eprint/77981>

---

**Published article:**

Hoath, SD, Vadillo, DC, Harlen, OG, McIlroy, C, Morrison, NF, Hsiao, W-K, Tuladhar, TR, Jung, S, Martin, GD and Hutchings, IM (2014) *Inkjet printing of weakly elastic polymer solutions*. *Journal of Non-Newtonian Fluid Mechanics*, 205. 1 - 10. ISSN 0377-0257

<http://dx.doi.org/10.1016/j.jnnfm.2014.01.002>

---

## Inkjet printing of weakly elastic polymer solutions

Stephen D. Hoath<sup>1</sup>, Damien C. Vadillo<sup>2</sup>, Oliver G. Harlen<sup>3</sup>, Claire McIlroy<sup>3</sup>, Neil F. Morrison<sup>3</sup>, Wen-Kai Hsiao<sup>1</sup>, Tri R. Tuladhar<sup>4</sup>, Sungjune Jung<sup>5</sup>, Graham D. Martin<sup>1</sup> and Ian M. Hutchings<sup>1</sup>.

<sup>1</sup> University of Cambridge, Department of Engineering, Institute for Manufacturing, 17 Charles Babbage Road, Cambridge, CB3 0FS, UK; corresponding author is SDH: T +44 1223 764626 F +44 1223 464217 E [sdh35@cam.ac.uk](mailto:sdh35@cam.ac.uk) +44(0)1223764626

<sup>2</sup> University of Cambridge, Department of Chemical Engineering & Biotechnology, New Museums Site, Pembroke Street, Cambridge, CB2 3RA, UK; current address AkzoNobel Research, Development and Innovation, Stoneygate Lane, Felling, Gateshead, NE10 0JY, UK.

<sup>3</sup> University of Leeds, School of Mathematics, Woodhouse Lane, Leeds LS2 9JT, UK

<sup>4</sup> University of Cambridge, Department of Chemical Engineering & Biotechnology, New Museums Site, Pembroke Street, Cambridge, CB2 3RA, UK; now at Trijet Ltd, 59 Eland Way, Cambridge, CB1 9XQ UK. [tuladhar@cantab.net](mailto:tuladhar@cantab.net) +44(0)1223474429

<sup>5</sup> University of Cambridge, Department of Engineering, Institute for Manufacturing, 17 Charles Babbage Road, Cambridge, CB3 0FS, UK; now Department of Creative IT Engineering, Pohang University of Science and Technology, South Korea

## **Abstract**

Fluid assessment methods, requiring small volumes and avoiding the need for jetting, are particularly useful in the design of functional fluids for inkjet printing applications. With the increasing use of complex (rather than Newtonian) fluids for manufacturing, single frequency fluid characterisation cannot reliably predict good jetting behaviour, owing to the range of shearing and extensional flow rates involved. However, the scope of inkjet fluid assessments (beyond achievement of a nominal viscosity within the print head design specification) is usually focused on the final application rather than the jetting processes. The experimental demonstration of the clear insufficiency of such approaches shows that fluid jetting can readily discriminate between fluids assessed as having similar LVE characterisation (within a factor of 2) for typical commercial rheometer measurements at shearing rates reaching  $10^4 \text{ rad s}^{-1}$ .

Jetting behaviour of weakly elastic dilute linear polystyrene solutions, for molecular weights of 110-488 kDa, recorded using high speed video was compared with recent results from numerical modelling and capillary thinning studies of the same solutions. The jetting images show behaviour ranging from near-Newtonian to “beads-on-a-string”. The inkjet printing behaviour does not correlate simply with the measured extensional relaxation times or Zimm times, but may be consistent with non-linear extensibility  $L$  and the production of fully extended polymer molecules in the thinning jet ligament.

Fluid test methods allowing a more complete characterisation of NLVE parameters are needed to assess inkjet printing feasibility prior to directly jetting complex fluids. At the present time, directly jetting such fluids may prove to be the only alternative.

## **Keywords**

Inkjet, polymer solutions, viscosity, elasticity, finite extensibility, beads-on-a-string.

## **Highlights**

- High speed images of weakly elastic polymer inkjets with beads-on-a-string
- Behavior of mono-disperse polystyrene solution jets vs. molecular weight
- Jetting behavior consistent with production of fully stretched molecules
- Inkjet fluid assessments based on linear viscoelasticity prove insufficient.

## **Abbreviations**

LVE Linear viscoelastic

NLVE Non-linear viscoelastic

## 1. Introduction

Inkjet printing involves jetting some liquid material through a nozzle opening to form drops with enough forward speed to reach a substrate at  $\sim 1$  mm “stand-off” distance. Drop production can be tailored to liquid properties using piezo print head actuation timing, but optimum conditions are very often determined by empirical trial and error. Newtonian fluids that can be usefully jetted from a given print head have a rather narrow range of properties, certainly within factors of 10, usually within factors of 2. In practice, print heads may be operated at a raised temperature to attain the optimum values of fluid properties (e.g. viscosity) that lie outside the jetting range at ambient.

With the projected interest in using complex (rather than Newtonian) inkjet fluids for manufacturing [1], such as functional fluids for flexible electronics and solar cells, effective fluid assessment techniques are of great interest. Demonstrations of links between rheology, drop formation and inkjet printing for linear polymers in solution have already shown [2] that single characterisation parameters such as the low shear rate viscosity do not provide sufficient indicators to assess good jetting behaviour.

This finding might seem unsurprising to fluid mechanics specialists in that jetting is an inherently non-linear process, but many empirical outcomes for drop-on-demand (DoD) inkjets appear straightforward and linearly predictable. Perhaps, because of this deceptive simplicity, the majority of fluid assessments prior to attempting inkjet printing are usually focused on the final application rather than on jetting processes. Typical deformations of the piezo producing the jet are small compared to the nozzle width (20 nm against 30  $\mu\text{m}$ ), so the linear viscoelastic (LVE) response of the fluid might well have an effect; fluids of similar LVE may reveal non-linear jetting effects.

So, provided nominal properties can be achieved lying within the print head design specification, application and ink formulation engineers concentrate on deposition. Those more concerned with the jetting issues have pursued inkjet fluid assessments via rheological measurement. Our previous paper on links between rheology, DoD drop formation and inkjet printing [2] provides guidance on optimising jetting performance, based on measurements of LVE moduli and complex viscosity. Attempts have also been made to understand limits to jetting of dilute solutions of polystyrene observed in our experiments [3] and those of de Gans *et al* [4], which led to consideration of non-linear viscoelastic (NLVE) effects in the DoD jetting process.

The interplay between the extensional rate  $U/D$  for jet speed  $U$  and nozzle diameter  $D$ , the longest Zimm relaxation time  $\lambda_Z$  and the finite extensibility  $L$  for the polymer weight  $M_w$  in the solvent viscosity  $\eta_s$  and the corresponding solvent quality factor  $\nu$ , appear to be key factors determining the jetting behaviour of high (100-1000 kDa) molecular weight polymer solutions, as discussed by Hoath, Harlen and Hutchings (HHH) [3], who developed a simple DoD model prompted by Bazilevskii, Meyer and Rozhkov [5]. HHH provides estimates of the jet head slowing down in three regimes of jetting behaviour for polymer molecules, corresponding to the Newtonian low shear-rate viscosity in which the polymers remain close to their equilibrium conformation, a viscoelastic liquid in which the polymers become extended but then subsequently relax, or a liquid in which the polymers become fully extended resulting in an extensional viscosity  $\sim L^2$  greater than the Newtonian low shear-rate viscosity. The filament thinning action before main drop detachment (“break-off”) from the

nozzle meniscus reduces the effects of the high extensional viscosity on the final drop speed by a factor of  $L$ . This “fully-stretched” regime predicts that higher polymer concentrations can be DoD jetted than predicted on the basis of a viscoelastic response with relaxation, which was unexpected and unreported prior to HHH.

McIlroy, Harlen and Morrison [6] relaxed several assumptions in the HHH model and enlarged the predictions for polymer jetting to explain the observations, by A-Alamry *et al* [7], of polymer molecule scission in DoD jetting. Partial unraveling of polymer molecules (“pre-stress”) within the jetting DoD nozzle was identified as a key aspect explaining experimental results in HHH. These papers have provided an improved level of confidence in the interpretation of DoD jetting results and experiments obtained with a variety of print heads, polymer fluids and solvents, for example those described de Gans *et al* [4] and A-Alamry *et al* [7]. Interestingly here, the improved modeling [6] showed that the intermediate viscoelastic regime is masked, suggesting that extensional properties might prove useful indicators of the DoD jetting behaviour.

The present work reports the DoD jetting behaviour of the series of weakly elastic linear polystyrene (PS) in diethyl phthalate (DEP) solutions that were recently assessed using filament thinning techniques by Vadillo, Mathues and Clasen (VMC) [8], with a view to investigating the role of NLVE parameters in DoD inkjet printing. A brief summary of recent results reported by VMC and others closes this section.

Polymers introduce startlingly new physics [5, 9-13] into purely Newtonian fluid flow behaviour. Attempts to provide a simple method for evaluating fluids intended for DoD inkjet printing have already shown [2, 14] that simple low ( $< 10^2 \text{ s}^{-1}$ ) shear-rate viscosity measurements are insufficient to characterize jetting performance. The LVE (moduli  $G''$  and  $G'$ ) determined at high frequencies ( $> 10^3 \text{ s}^{-1}$ ) are relevant to the DoD jetting performance as the repetition frequency of the piezoelectric drive pulses is typically  $10^4 \text{ s}^{-1}$  [15].

For mono-disperse PS solutions in DEP the relaxation times obtained from LVE,  $\lambda_0$ , are found to approach the Zimm time  $\lambda_Z$  in the dilute limit, with the ratio  $\lambda_0/\lambda_Z$  increasing as the concentration approaches  $c^*$  (the critical concentration) as a function of the reduced concentration  $c/c^*$  independent of molecular weight [12]. However the extensional relaxation times  $\lambda_E$  obtained from filament thinning [16] were found by VMC to have a much stringer concentration dependence. They reported values of  $\lambda_E$  for low molecular weight  $M_W < 220 \text{ kg mol}^{-1}$  that were much longer than the Zimm times  $< 20 \text{ }\mu\text{s}$ . Hence even at concentrations  $c/c^* < 0.1$  polymeric additives would be expected to lengthen filament thinning times during drop break-off in inkjet printing. Consequently the extensional relaxation time is an important determinant for inkjet performance.

Capillary thinning and related approaches might be considered as providing necessary assessment tools for characterising inkjet printing fluids, but their sufficiency has not yet been quantitatively demonstrated by inkjet experiments, despite the success enjoyed by some recent numerical simulations of polymeric fluid jets [17]. Mechanical stretching has slower timescales (by factors of 10-100) and larger linear size (by similar factors) than for DoD jetting. To test for correlations between thinning and jetting the present experimental work compares jetting behaviour of weakly elastic polymer solutions of mono-disperse PS in DEP with similar (within a

factor of 2) low frequency properties shown in Figure 1 [10]. PS solutions are indicated herein by their molecular weight ( $M_w$ ) in  $\text{kg mol}^{-1}$  (e.g. PS110).

Figure 1 shows these VMC fluids ( $c/c^* \sim 0.1$ ) have similar zero shear viscosity  $\eta_0$  and LVE response in the range  $10^2$ - $10^4$   $\text{rad s}^{-1}$  where it can be measured using a piezo axial vibrator (PAV) [18,19]. At low frequency,  $G'' \sim \eta_0 \omega$  while  $G' \sim G \lambda^2 \omega^2$ , so the VMC fluids were chosen such that  $G \lambda^2 \sim \text{constant}$ . This was a compromise between keeping  $c/c^*$  roughly constant so that values of  $\eta_0$  and  $G''$  are the same, but in practice this decreases by a factor of 2 as  $M_w$  increases between 110-488  $\text{kg mol}^{-1}$  - and fixing  $G \lambda^2$  - which increases by a factor of 1.5 as  $M_w$  increases from 210-488  $\text{kg mol}^{-1}$ . In addition, fitting a multi-mode Zimm model [8] to the VMC data as shown in Figure 1 implies bigger differences between different solutions occur at high ( $> 10^4$   $\text{s}^{-1}$ ) frequencies which might prove significant for inkjets.

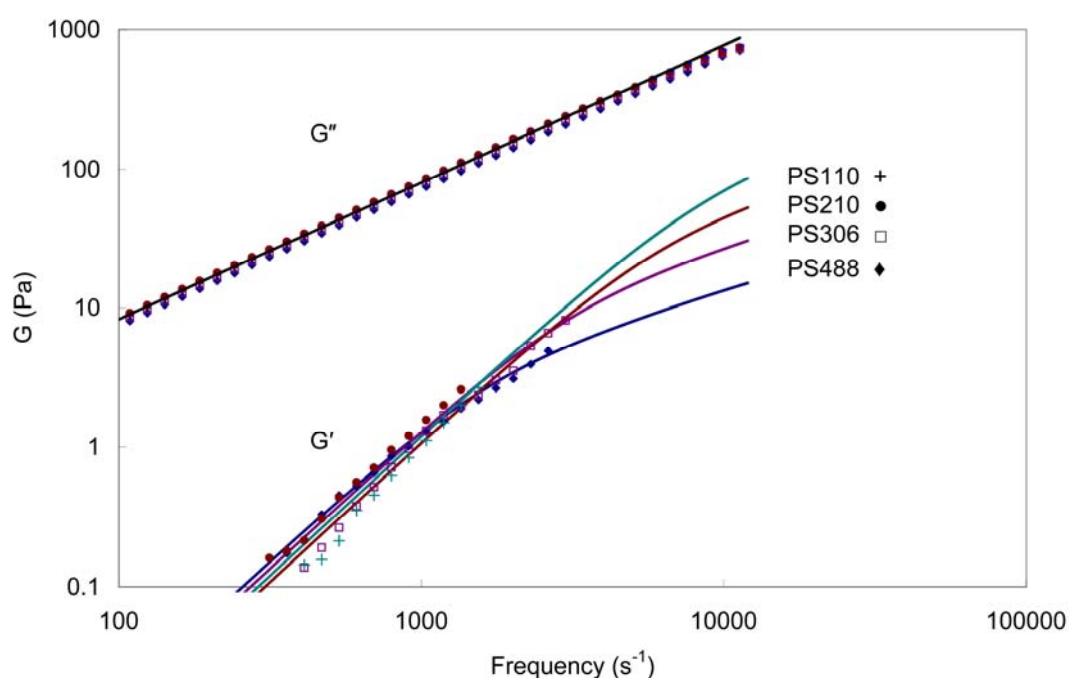


Figure 1. Elastic  $G'$  and storage  $G''$  moduli (measured using PAV) for the PS in DEP solutions of Vadillo, Mathues and Clasen that were jetted in the present work. Fits to the  $G''$  data for PS110 and predictions of multi-mode Zimm models for  $G'$  data are shown [8].

VMC reported, as shown in Figure 2, that the ratio of the linear relaxation time ( $\lambda_0$ ) to  $\lambda_Z$  varied with the reduced concentration  $c/c^* > 0.015$  for the PS in DEP fluids independently of  $M_w$ . Figure 2 extrapolates the asymptotic value of  $\lambda_0/\lambda_Z$  from low to high  $c/c^*$  and compares the exponential predictions of the Martin equation [8] and a quadratic fit to the data [6]. For PS solutions with  $c/c^* \sim 0.1$ , as used in the present work, Figure 2 suggests values of the ratio  $\lambda_0/\lambda_Z$  would always lie between 1 and 1.5.

In marked contrast, VMC observed the ratio of extensional relaxation time  $\lambda_E$  to Zimm time  $\lambda_Z$  reduced with increasing  $M_w$ , with  $\lambda_E$  being a factor 25 larger than  $\lambda_Z$  for the PS110 solution, a factor 4.6 larger than  $\lambda_Z$  for the PS210 solution, but very similar to  $\lambda_Z$  for the PS306 and PS488 solutions. Possible roles for the extensional relaxation times of PS solutions measured by VMC in explaining DoD jetting behaviour of the same PS solutions are examined later in the discussion section.

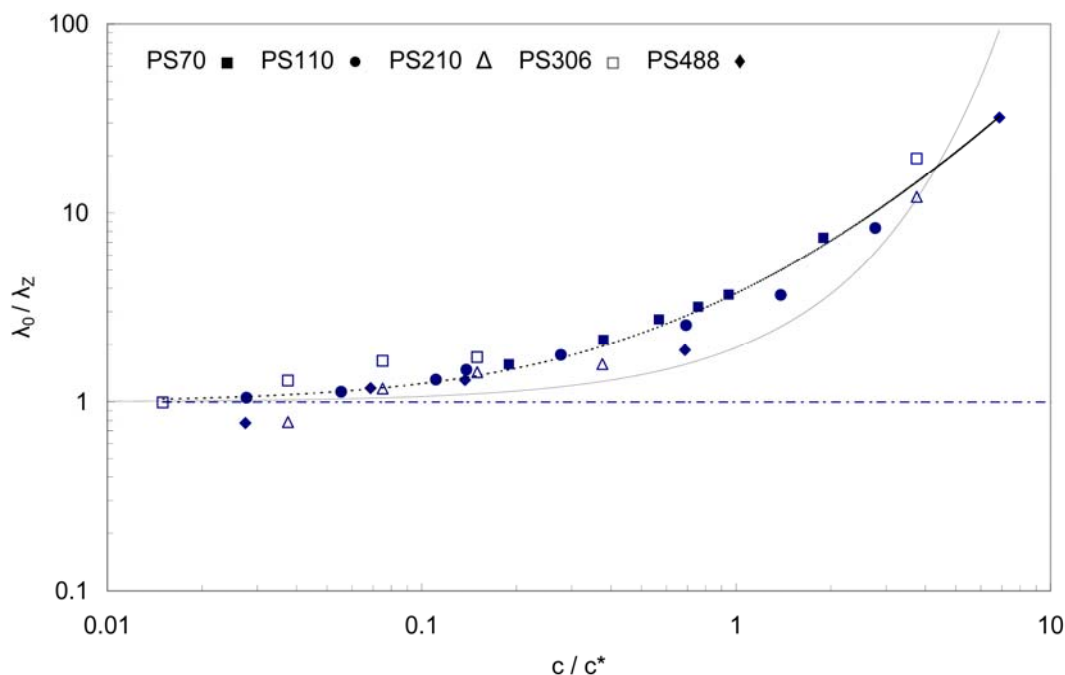


Figure 2. The ratio of reduced relaxation time to the Zimm relaxation time,  $\lambda_0/\lambda_z$ , for PS in DEP from VCM data [8] as a function of reduced concentration  $c/c^*$ . (See text.)

The linear viscoelastic response of these solutions is independent of the associated finite extensibility ( $L$ ). However, in recent studies of high speed ( $\sim 6 \text{ m s}^{-1}$ ) jetting of PS solutions in DEP we have found experimental and theoretical evidence [3, 6] for the influence of  $L$ . Consequently, differences in the jetting behaviour between fluids with “similar” VLE response may result from the influence of the polymer extensibility. Szabo, McKinley and Clasen [20] have recently investigated a method for measuring  $L$ .

In a recent paper Yoo and Kim [21] has also considered the roles of rate dependent shear and elongational viscosity in DoD drop formation along with the flows of ink inside a MicroFab nozzle with  $50 \mu\text{m}$  exit diameter. They studied filament thinning of Xanthan gum in various water-glycerin mixtures as model fluids exhibiting shear thinning behaviour. Primary drop speeds (and ejected volumes) were found to be linear in drive voltage, and decrease with the low shear viscosity, as previously reported [22, 23]. Importantly, since for these model fluids the elastic modulus  $G'$  is far smaller than the viscous modulus  $G''$  up to  $10^5 \text{ rad s}^{-1}$ , the model fluid behaviour in DoD drop generation is certainly not elastic [21].

Such results suggest that polymer relaxation time and finite extensibility may control inkjet printing at high jet speed. For the present work, “similar” PS polymer solutions at fixed drive voltages from an inkjet print head have been video recorded at high speed ( $500,000 \text{ frame s}^{-1}$ ) to provide characteristic information about fluid jetting, e.g. in-flight speed variation, ligament thinning, growth of primary and secondary beads formed on the ligament [24, 25], the time and ligament length at “break-off” from the nozzle meniscus (and subsequent ligament break up) for comparison, analysis and interpretation of these observations.

It is important to note here that different mechanisms may be responsible for the slowing down of the drop as opposed to the jet break-off from the nozzle meniscus. Drop break-off is local and driven by the local balance between surface tension and what become fully extended polymers [6], whereas the slowing down of the main drop is due to the tension in the filament [3]. On average the polymer extension in the filament at first stretches and then relaxes as the extension-rate drops below the critical value, however at the point of local thinning the extension-rate remains sufficient to fully extend the polymer molecules. Therefore in the later discussion of the jetting experiments there may be different factors controlling the observed break-off times and final drop speeds: each jetting data set is mapped against the individual NLVE parameters  $\lambda_z$  and  $L$ .

## 2. Experimental

Weakly elastic polymer solutions of mono-disperse polystyrene in diethyl phthalate as a good solvent [2, 3, 8] were prepared at various molecular weight values ( $M_w$ ) and wt% concentration ( $c$ ) as listed in Table 1 [8]. These dilute PS in DEP solutions were deliberately prepared to have reasonably matched LVE properties for frequencies up to  $10^4$  rad s<sup>-1</sup> (see Figure 1) giving similar values for  $\eta^*$ , while due to their different molecular weights they have different Zimm times ( $\lambda_z$ ) and extensibilities ( $L$ ). Previous work [3] had shown that the polystyrene polymer concentrations ( $c$ ) used were a factor of 10 below the critical concentration limit ( $c^*$ ) – see Table I. The linear viscoelastic parameters used to determine complex viscosity  $\eta^*$  were found using the piezo-axial vibrator (PAV) technique that is fully described elsewhere [18, 19].

$M_w$ (kg / mol)	$c$ (wt%)	$c/c^*$ (-)	$\eta^*$ (mPa s)	$\eta$ (mPa s)	$\lambda_z$ ( $\mu$ s)	$L$ (-)
110	0.50	0.134	13.2	12.4	7.8	14.8
210	0.40	0.143	13.0	12.5	20.0	21.3
306	0.20	0.080	12.0	11.6	32.9	25.2
488	0.10	0.065	11.7	11.0	83.8	31.0

**Table I:** Characteristic parameters of the jetted polystyrene in diethyl phthalate solutions [8].

The fluids were jetted from a MicroFab (MF) inkjet nozzle with 30  $\mu$ m exit diameter. The nozzle was purged by jetting with pure DEP between each solution type to avoid cross-contamination. A MF JetDrive III controller bipolar “pull-push” waveform [15] (with fixed 2  $\mu$ s rise and fall times, 10  $\mu$ s “pull” time and 20  $\mu$ s “push” time) was used for each solution to permit fair cross comparison of the fluid jetting behaviour at fixed drive voltage, although images were also recorded at other drive voltages as a systematic cross-check. The jetting image comparisons shown here were recorded at drive voltages of 35V and 32V, the higher voltage being sufficient to ensure that all the polymer solutions produced a main drop with positive velocity.

Figure 3 shows a schematic for our shadowgraph inkjet imaging system using an ultra high speed camera [26] and long duration ( $\sim$  2 ms) high power flash lamp to illuminate the flight path. Jets from the MF nozzle exit lie in the focal plane of a Shimadzu HPV-1 ultra high speed camera (EPSRC Engineering Instrument Loan Pool

#2) coupled to a Navitar  $\times 12$  telescope with Mitutoyo  $\times 10$  NA = 0.28 objective lens. The high power flash lamp (with adjustable iris and focussing lens) was driven by an Adept Electronics CU-500 controller. The recharging rate of the flash lamp power supply limited the sequence recording rate to a maximum of  $\sim 20$  triggers every 15 minutes, but suitable allowance could be made by using the recovery time for fluid changes and system purges as discussed above. When recording was required, the Shimadzu software was primed to respond to an external trigger and then a manual trigger was applied to a pulse/delay generator which provided external triggering to the MicroFab JetDrive III controller, flash controller and Shimadzu HPV-1 camera.

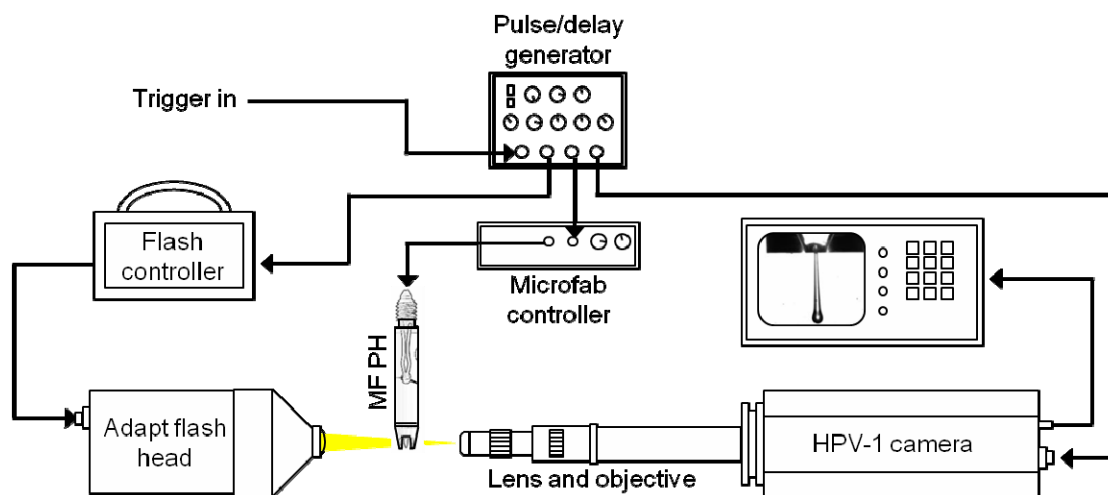


Figure 3: A schematic layout for the experimental set up used in the present work.

The Shimadzu HPV-1 camera system was operated at 500,000 frames per second providing a  $312 \times 260$  pixel resolution. The camera stored sequences of 102 frames, corresponding to  $202 \mu\text{s}$  elapsed time at this rate, that were normally triggered by the initiation of inkjet printing so as to capture jet emergence. A time delay of  $25 \mu\text{s}$  corresponded to a jet tip just leaving the MicroFab nozzle exit. For the higher  $M_W$  an extra  $175 \mu\text{s}$  delay was used to capture events delayed beyond 102 normal frames.

A  $\frac{1}{2} \mu\text{s}$  exposure time (=  $\frac{1}{4}$  frame duration) reduced blurring of the fast jet images. (The earlier images frames were under-exposed but event histories were unaffected.) The linear calibration was determined off-line from the known nozzle dimensions, since the whole end face and outer wall of the MicroFab device were always imaged together with the jetted fluid. The linear calibration was  $4.26 \mu\text{m}$  per pixel: the camera was oriented and aligned to image jets and drops within  $\sim 0.92 \text{ mm}$  of the nozzle exit. This linear calibration was used with the frame timing to determine the drop tip speed.

These jetting experiments were conducted with an ink absorbing catcher mounted at least  $5 \text{ mm}$  below the print head nozzle exit. In typical inkjet printing applications the deposition substrate would be located  $1.0 \text{ mm}$  below the nozzle exit. Thus the field of view chosen for these experiments is appropriate for real inkjet applications.

### 3. Results

The higher molecular weight polymer solutions showed significantly delayed ( $>100$   $\mu\text{s}$ ) break-off and behaviour reminiscent of “beads on a string” formation [9]; the break-off of even the lowest molecular weight solution ( $M_w = 110$  kg/mol) was also delayed compared with a Newtonian fluid mixture of 10 wt% dioctyl phthalate (DOP) and 90 wt% DEP with similar viscosity  $\eta \sim 16$  mPa s to that of the complex viscosities  $\eta^*$  of Table I. These results are consistent with earlier results on DoD jetting of viscoelastic fluids from Bazilevskii *et al* [5].

Table II lists analyzed measured jet/drop speeds together with the break-off times and estimated break-off lengths for the fluid jets produced by 35V and 32V drive voltages. Break-off lengths were estimated from the known linear calibration of the images, ignoring the unknown length that could lie within the nozzle at the break-off time, while the speed of drops were determined from changes in the final few video frames. For higher  $M_w$  solutions (PS306 and PS488) the absolute values of break-off times include the extra 175  $\mu\text{s}$  recording delay needed to capture the break-off event at the same (500,000 fps) frame rate as for the other solutions (DOP/DEP, PS110 and PS210). The speed of the PS488 drop at 32V drive is negative, corresponding to the main drop moving back towards the nozzle that clearly would be unacceptable in inkjet printing applications.

Jetted at (32 V) 35 V	DOP/DEP 10%/90%	PS110 0.5wt%	PS210 0.4wt%	PS306 0.2wt%	PS488 0.1wt%
Break-off time ( $\mu\text{s}$ )	(62) 60	(102) 104	(198) 194	(> 227) 225	(309) 303
Break-off length ( $\mu\text{m}$ )	(470) 620	(440) 580	(590) 810	(350) 570	(380) 770
Speed of drop (m/s)	(3.6) 8.4	(2.2) 3.6	(1.4) 2.3	(0.5) 1.4	(-0.5) 0.6
Bead ( $\mu\text{s}$ ) formation	(> 170) > 170	(130) 150	(150) 140	(150) 160	(190) 180

**Table II:** Break-off times and drop speeds at 35 V (32 V) drive recorded for a viscous Newtonian fluid DOP (10%)/DEP(90%) and for the same weakly elastic polymer solutions as studied by VMC [8]. The results at 32V drive are shown in brackets for comparison purposes. (See text for further details.)

Figures 4-8 each show jetting image sequences in successive 10  $\mu\text{s}$  strips (with labels every 20  $\mu\text{s}$ ) corresponding to 35V and 32V drive voltages for the Newtonian DOP/DEP solution and the four PS in DEP solutions of Table I. Extraneous light variations have been grayed out in all sequences and shown with a linear guide edge. The nozzle exit was located just above the top of each strip (0.92 mm of flight path).

Figure 4 shows the viscous Newtonian fluid at (a) 32 V and (b) 35 V drive voltage. As expected, the viscous Newtonian fluid produced at least one satellite as the fluid body moved forwards at 32 V drive. With a drive of 35 V the ligament breaks first near the nozzle and then just behind the drop head. Although final drop speeds and break-off lengths are quite different for the two drive voltages, the break-off times for

these conditions were within a single  $2\mu\text{s}$  time frame, as given in Table II above. The tail speeds are similar for the different drive voltages, although the head speeds differ, as well-known for Newtonian fluids, e.g. as reported by Dong, Carr & Morris [27].

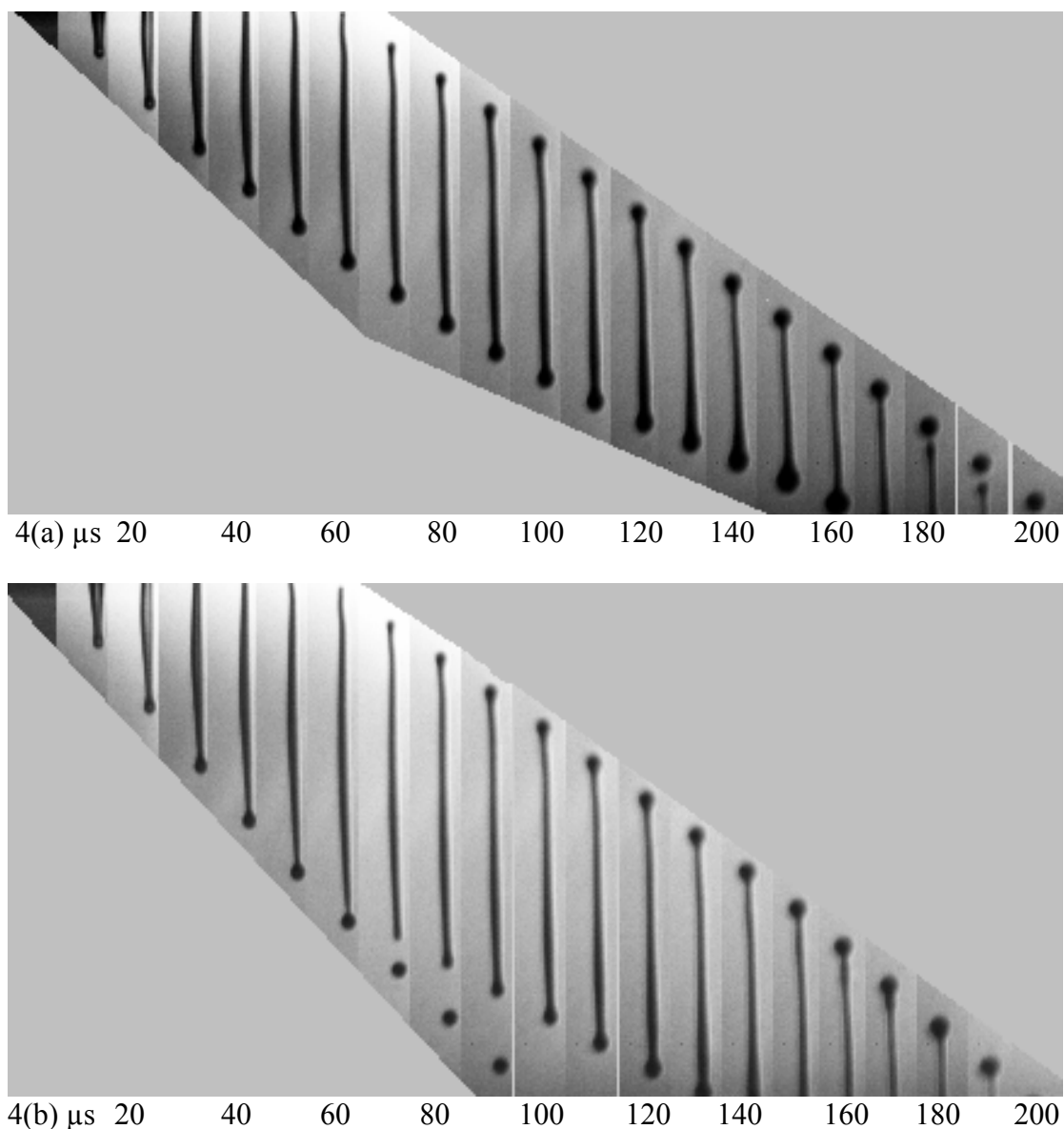


*Figure 4. Jetted Newtonian 10wt% DOP 90wt% DEP solution at (a) 32 V and (b) 35 V drive voltage. The ligament breaks behind the main head in (b) for the higher drive voltage (faster jet), while break-off times and end tail speeds are similar for (a) & (b).*

Figure 5 shows the corresponding image sequences for the PS110 solution at (a) 32 V and (b) 35 V drive voltage. While the influence of the added polymer compared with the Newtonian solution is to slow down the head motion significantly for both drive voltages, a single drop formed for 32 V drive whereas multiple unmerged drops were produced at 35 V. The sequence shows that the jet ligament shortens and eliminates satellites in (a) but necks form in several locations that produce some satellites in (b): head speed controls this. There is evidence for thin tails and ligament in (b), which were short lived ( $< \sim 20\mu\text{s}$ ). The trailing ligament appears to be slightly conical until break-off from the nozzle, which occurs at similar times for both voltages.

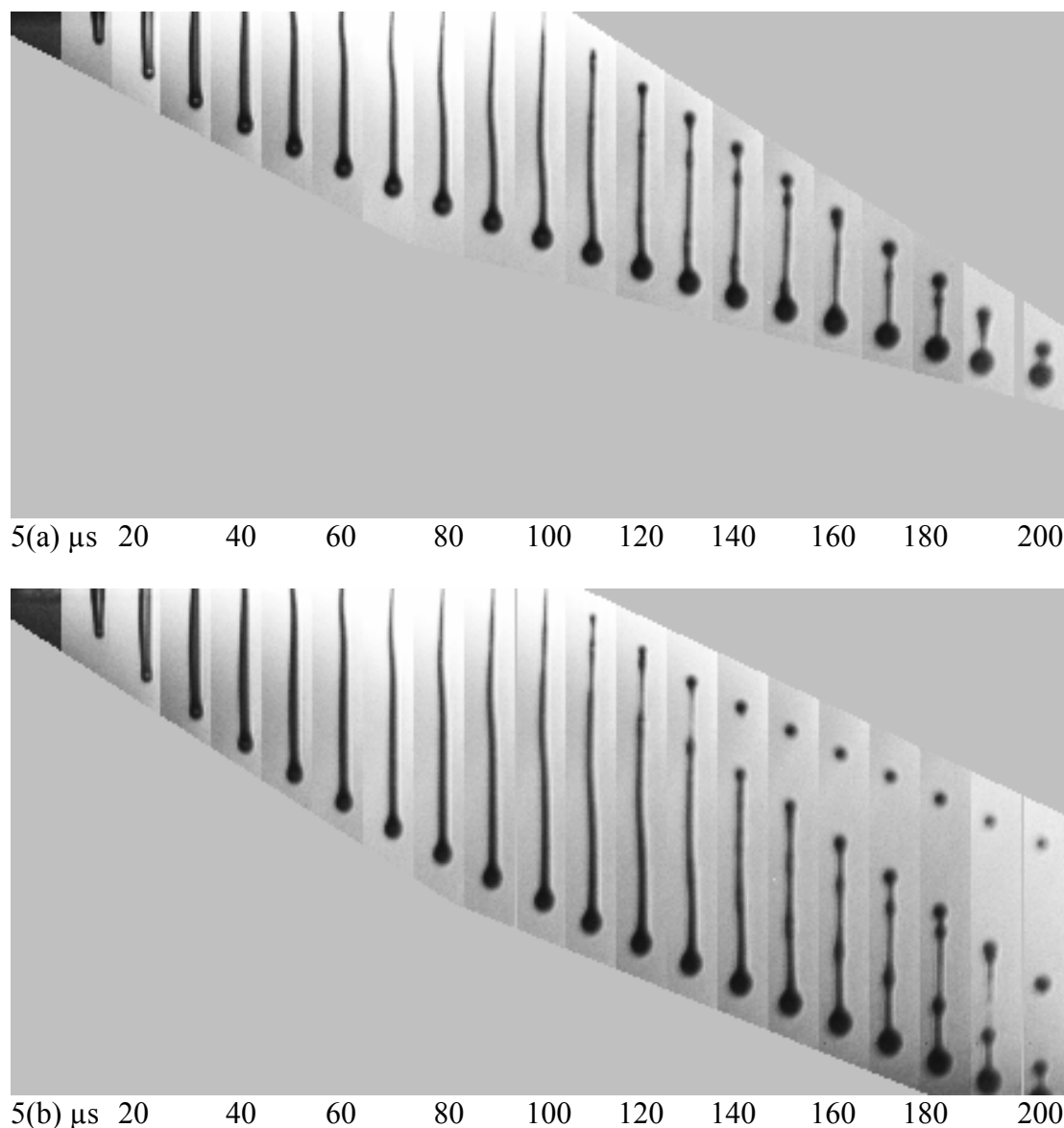


Figure 5. Jetted 0.5 wt% PS110 in DEP at (a) 32 V and (b) 35 V drive voltage.

Figure 6 gives corresponding image sequences for the jetted 0.4 wt% solution of PS210 in DEP at (a) 32 V and (b) 35 V drive voltage. The jet slows down significantly and beads begin to form before break-off for the 32 V drive voltage, but the main drop moved forwards as the ligament and satellite drops merged with it; at 35 V the same pattern was seen with multiple satellite “beads on a string” behind. The ligament appears cylindrical until it necks down. Beads move along the thread and then merge, either with other beads or the head. Again, the break-off occurs at rather similar times for both voltages and noticeably later than evident for the jetted 0.5 wt% PS110 in DEP in Figure 5 above.

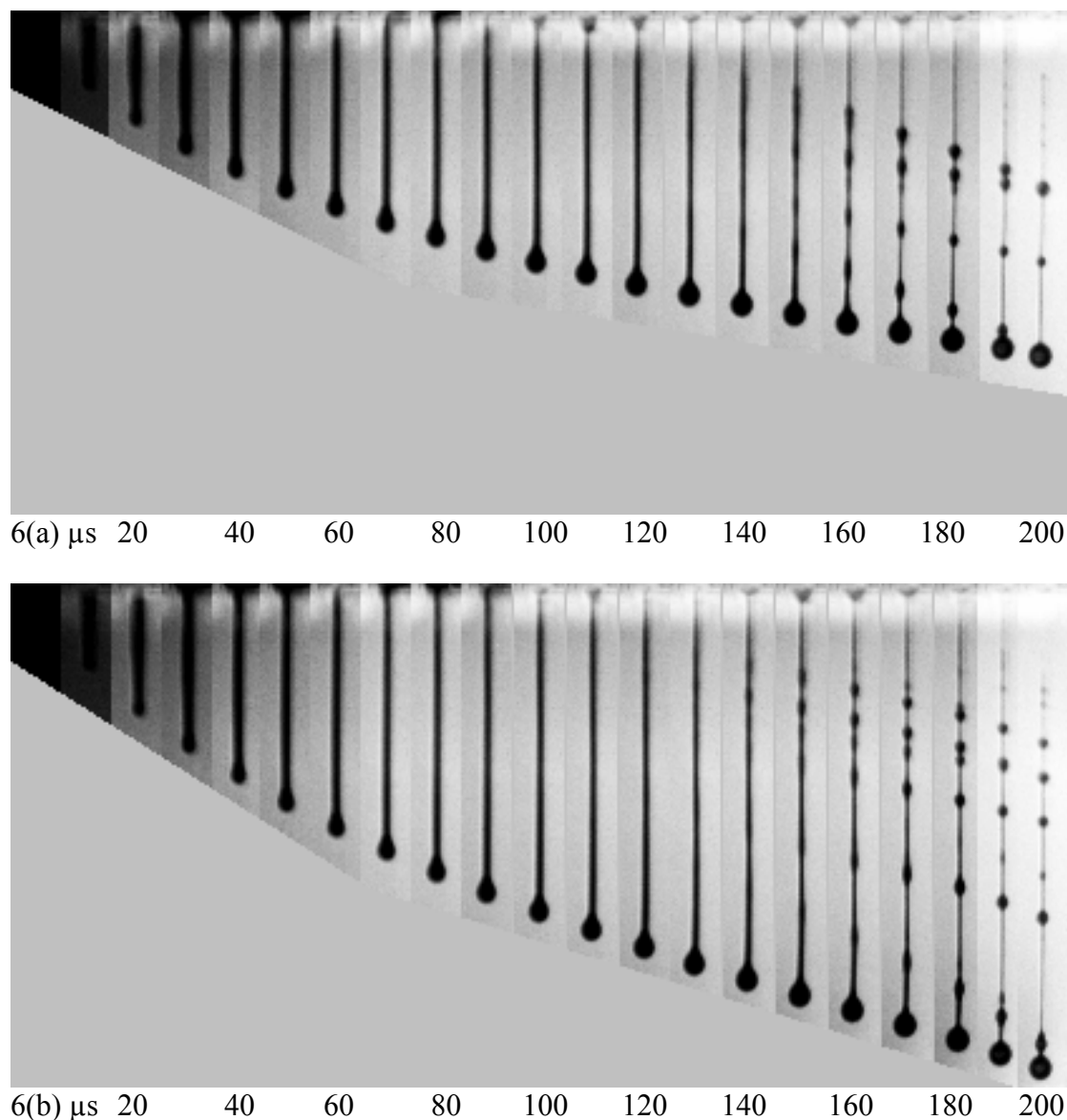


Figure 6. Jetted 0.4 wt% PS210 in DEP at (a) 32 V and (b) 35 V drive voltage.

Figure 7 shows the corresponding image sequences for jetted 0.2 wt% PS306 solution at (a) 32 V, (b) 35 V and (c) 35 V drive voltage (delayed 175  $\mu\text{s}$  and corresponding to a different jetting event.) Significant slowing down of the head is occurring in (a) well after the jet has emerged from the nozzle, with the jet forming almost stationary drop with a long beaded ligament. Inspection of (b) and (c) at similar times show reproducible jetting behaviour at 35 V drive voltage: the slowing down of the emerging head is evident in (b). In (c) the jet produces a slow main drop and a faster following large satellite drop. The ligament threads thin and rupture earlier at the end closest to the nozzle. Also just visible in the sequence (c) is a much smaller trailing satellite drop that originated in the thinning ligament between a satellite drop and ink in the nozzle. The break-off times appeared to be reasonably consistent, although only an estimate for 32 V drive voltage could be determined from the image sequence (a).

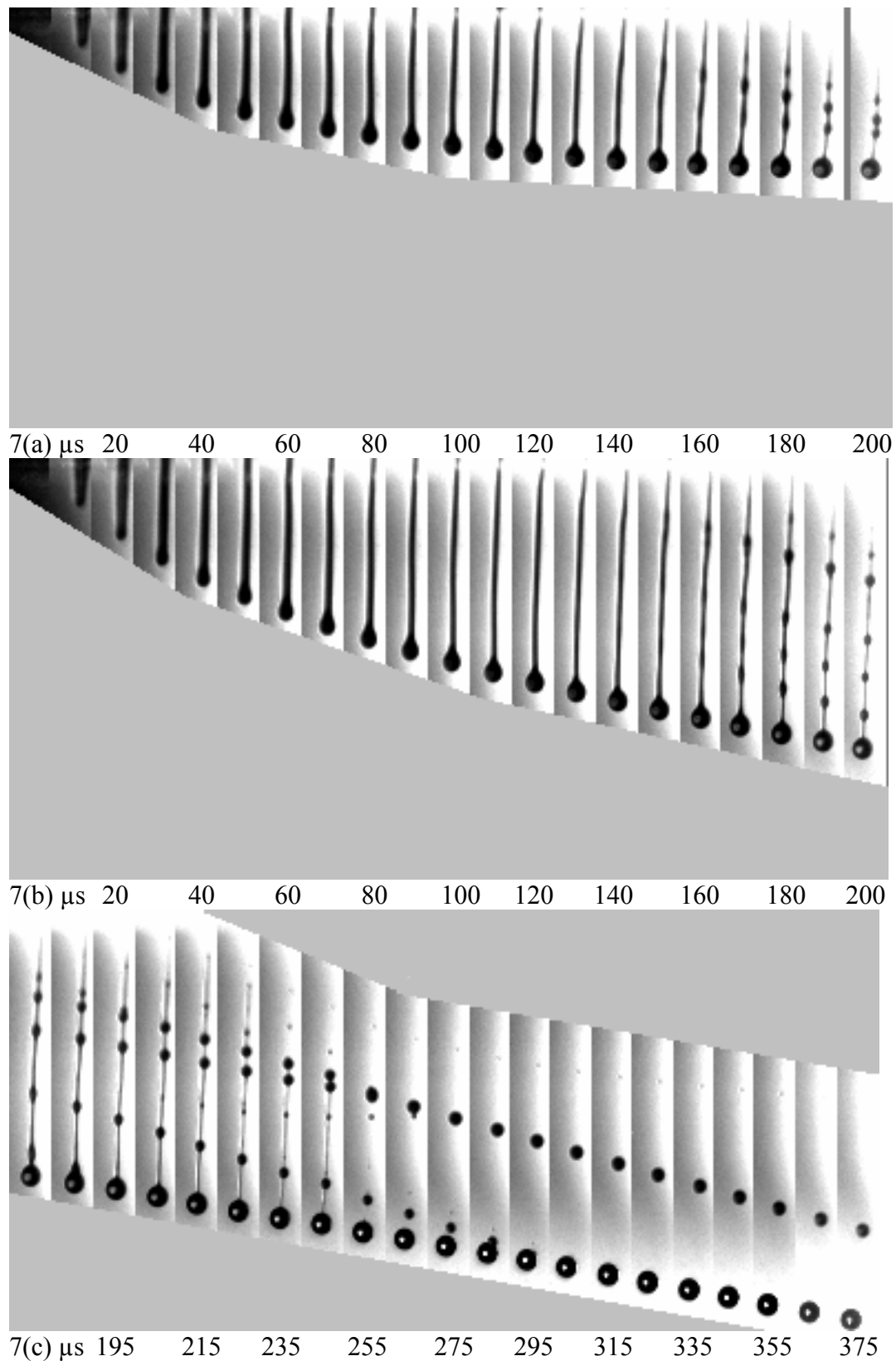


Figure 7. Jetted 0.2 wt% PS306 in DEP jetted at (a) 32 V and (b) & (c) 35 V drive voltage. The delayed jet in 7(c) corresponds to a different jet event from that in 7(b).

Figure 8 shows the jetting image sequences for the 0.1 wt% PS488 solution at (a) 32 V (delayed 175 $\mu$ s), (b) 35 V and (c) 35 V (delayed 175 $\mu$ s). At 32 V drive voltage the main drop head had already started to move back (recoil) towards the nozzle before the ligament broke centrally and the head then continued moving back after break-off. (The upwards recoil of the drop in Figure 8(a) reflects the relative weakness of gravity on short ( $\sim 200 \mu$ s) timescales of DoD inkjet printing. See also discussion of drops speeds in inkjet printing [23].)

At 35 V drive voltage, sequence (c) shows that multiple droplets were forming on the ligament which also snapped centrally, with the main drop and some satellites still moving slowly forward but with the satellites on the nozzle side of the break moving backwards. The “beads on a string” form satellites that all clearly move away from the “mid-point” location of the ligament. The observed break-off times for PS488 solution at the 2 different voltages were quite (2%) comparable and were five times longer than the Newtonian fluid break-off times in Table II.

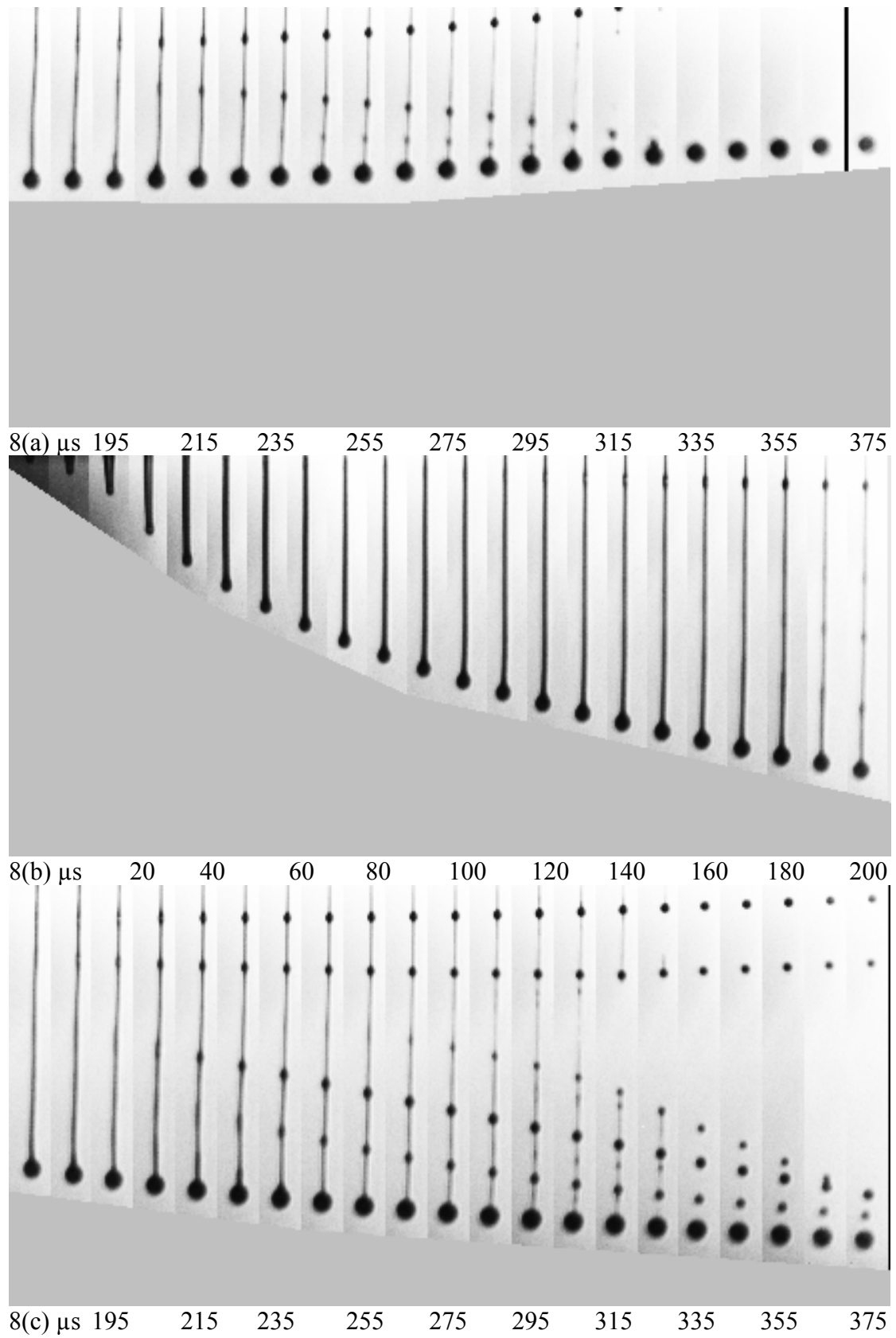


Figure 8. Jetted 0.1 wt% PS488 in DEP at (a) 32 V (b) & (c) 35 V drive voltage.

To aid the later discussion, Figure 9 represents the data recorded in Table II against PS molecular weight  $M_W$ , with Newtonian results plotted at  $M_W = 0$ . The fitted curves in Figure 9 are purely empirical and intended to guide the eye. The average time for the onset of beads formation ( $\blacktriangle$ ) and the observed break-off times for the 35 V ( $\bullet$ ) and 32 V ( $\circ$ ) drive voltages are shown in Figure 9(a). There is no strong variation of beads formation time with  $M_W$ , and in addition the results are almost independent of drive voltage. Jet break-off times, in contrast with the beads formation times, increase monotonically with increasing  $M_W$ , while also being independent of drive voltage. Figure 9(b) shows final drop speeds, where positive (negative) values correspond to downwards (upwards) motion. The large gap between the Newtonian drop speeds for the 35 V ( $\blacklozenge$ ) and 32 V ( $\circ$ ) drive evident in Figure 9(b) arises because for 35 V drive the drop head quickly broke off from the trailing Newtonian ligament in Figure 4(b). Therefore this 35 V speed results from a different process than in polymer jet slowing and is plotted separately. The final polymeric drop speeds tend to decrease at fixed drive voltage as  $M_W$  is increased even though the polymer concentration and solution viscosity is decreased. This contrasts with the systematic speed reduction with increasing polymer concentration at fixed polymer  $M_W$  and drive voltage [5].

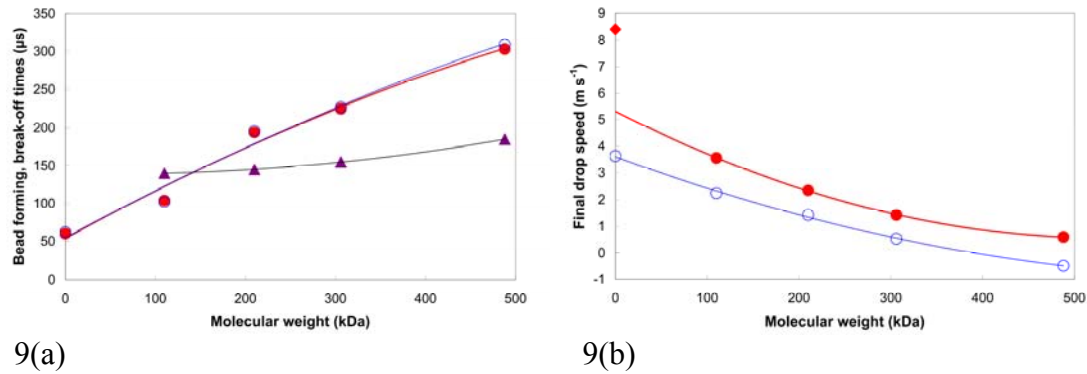


Figure 9 plots for 35 V ( $\bullet$ ) and 32 V ( $\circ$ ) drive voltage (a) average time for bead-on-a-string formation ( $\blacktriangle$ ) and the jet break-off times, and (b) the final drop speeds, at each PS molecular weight from Table II. Newtonian values are shown at the PS molecular weight of 0 kDa; in Fig 9(b) the Newtonian final drop speed for 35 V ( $\blacklozenge$ ) is shown separately (see text). Positive (negative) final drop speed corresponds to downwards (upwards) motion from (to) the nozzle. The quadratic line fits shown for each drive voltage (average or series) merely guide the eye.

#### 4. Discussion

The results of the present study, shown in figure 9, demonstrate that increases in the molecular weight of the polymer additive lead to an increase in break-off time and decrease in drop speed, despite the decreasing concentration and consequent decrease in fluid viscosity (as shown in Table I). Consequently, the observed behavior must be a consequence of the non-Newtonian properties of the solutions and is therefore expected to be dependent upon the solution relaxation time,  $\lambda$  and potentially also other non-Newtonian parameters such as the finite extensibility  $L$  of the polymer. Therefore in addition to the Reynolds number  $Re$  and Weber number  $We$  there are at least two further dimensionless parameters required to characterize the jetting and break-off of these fluids; the Weissenberg number,  $Wi = (U/D)\lambda$  based upon the deformation rates induced by the DoD jetting process and the Deborah number  $De = \lambda/\sqrt{(\rho R^3/\sigma)}$ , that characterizes capillary thinning.

However, we first need to determine the appropriate value for the relaxation time  $\lambda$ , which might be either the Zimm relaxation time  $\lambda_Z$ , or alternatively the extensional relaxation time  $\lambda_E$  as determined by VMC [8]. In the case of the two largest molecular weight solutions, the two relaxation times are roughly equal, however, for the two lower molecular weight solutions,  $\lambda_E$  is significantly larger, and decreases with molecular weight between PS110 and PS306 fluids. In figure 10 we plot both relaxation times as a function of break-off time for both the 35 V and 32 V drive. The break-off times increase monotonically with Zimm time  $\lambda_z$  but independently of the drive voltages used within small ( $\pm 2 \mu\text{s}$ ) experimental errors (not shown). Such independence from the drive voltage is also commonly observed [27] for DoD jetting of Newtonian fluids, including the DOP/DEP solutions jetted in the present work. This demonstrates that the jet break-off process is controlled by capillary thinning and so is characterized by the Deborah number, rather than the Weissenberg number. Surprisingly, there is no clear correlation between the break-up time and  $\lambda_E$ . Indeed none of the trends in the measurements of figure 9, appear to be explained by  $\lambda_E$ . Further discussion of the break-off time is therefore restricted to consideration of the possible roles of the Zimm time  $\lambda_z$  (and the finite extensibility  $L$ ).

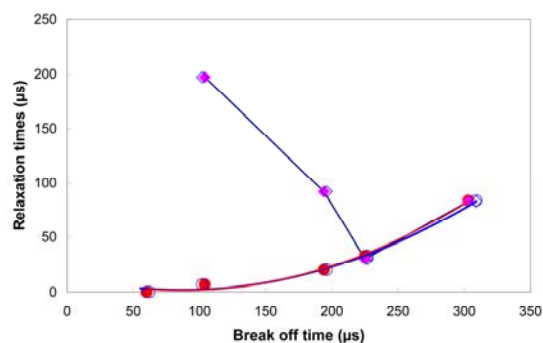


Figure 10 shows the Zimm times  $\lambda_z$  and the VMC extensional relaxation times corresponding to the break-off times found for the PS solutions at 35 V (●, ◆) and 32 V (○, ◇) drive voltage. The Newtonian solution break-off times are plotted at 0  $\mu\text{s}$  Zimm time. Curved trend lines guide the eye through the Zimm times (circles) for all five solutions, while straight lines connect the VMC extensional relaxation times (diamonds) for the four PS solutions (See text).

The independence of break-off time on drive voltage, suggests that the break-off process is driven by capillary thinning and should therefore follow the general theory for capillary driven break-off. The linear stability theory of Goldin *et al* [28] for the growth of the capillary instabilities on viscoelastic fluid jets, predicts a time  $\sim 67 \mu\text{s}$  for the growth of instabilities on a jet of radius  $R = 15 \mu\text{m}$  for a fluid of viscosity  $\eta \sim 16 \text{ mPas}$ , which is comparable to the observed DoD jet break-off times  $\sim 61 \pm 1 \mu\text{s}$  (Table II) at the 32 V and 35 V drive voltages used. However, this theory is not appropriate to the final stages of break-off when the instabilities become nonlinear. Break-off times for Newtonian fluid would be expected to follow the Eggers regime [29], based on Ohnesorge number  $Oh = 0.10$  for the DoD nozzle radius  $R = 15 \mu\text{m}$ , suggesting a rupture time of the order of 170  $\mu\text{s}$  under extensional flow. However this  $Oh$  number is sufficiently close to the critical value  $Oh = 0.20$  [30] that the radial necking speed lie between that for Eggers regime and the approximately 7/3 times

faster speed in the Papageorgiou regime [31]. The break-off time is then  $\sim 72 \mu\text{s}$  and also comparable with that seen for the Newtonian fluid jetted in the present work.

All the polymeric fluid jets have significantly longer break-off times, even though the low shear-rate viscosity values are slightly lower than that of the Newtonian fluid, from which a reasonable deduction is that the presence of polymer is resisting the break-off process. However, the break-off times do not correlate with the extensional relaxation times measured by VMC. Computing dimensionless Ohnesorge  $Oh = \eta/\sqrt{\rho\sigma R}$  and Deborah  $De = \lambda/\sqrt{\rho R^3/\sigma}$  numbers for the filament thinning geometry of the ‘‘Cambridge Trimaster’’ device and fluids of Table 1, VMC showed the initial conditions on 1.2 mm diameter scales are dominated by inertia, for which the break up timescales are  $\sim 5 \text{ ms}$  [10]. On  $30 \mu\text{m}$  nozzle diameter DoD jetting scales, the initial  $Oh \sim 1/2$  and  $De \sim 5$  for the polymer relaxation time of  $\sim 50 \mu\text{s}$ , which implies that the polymers will become extended during the jet thinning process [32].

For sufficiently high molecular weight polymer molecules there would be a regime of elasto-capillary balance where the filament thins exponentially on a timescale of  $3\lambda$ . For this regime to exist the polymeric stress must be able to balance the capillary pressure before the polymers become fully extended, which requires that  $L \gg (\sigma\lambda/\eta_p R_0)^{2/3}$ , where However, for the present DoD jetting experiments the concentrations and molecular weights are too small for this to be satisfied, meaning that the polymer molecules would become fully extended before elasto-capillary balance is achieved. Thus the initial Newtonian phase of drop break-off is followed by a linear radial shrinkage rate due to viscous fluid flow as described by Papageorgiou [31], with the fluid viscosity corresponding to extended molecules, which is a factor of  $\sim L^2$  greater than polymer contribution to the shear rate viscosity. However the radius below which this high viscosity applies is reached after axial extension by the factor  $L$ , and hence after the radius has reduced by factor  $1/\sqrt{L}$ . Thus the time taken for the polymer solutions to break-off during the Papageorgiou viscous dominated regime is proportional to  $L^{3/2}$ , independently of drop speed and drive voltage. The break-off time results at the 35 V ( $\blacklozenge$ ) and 32 V ( $\circ$ ) drive voltages from Table II are shown in Figure 11. The best fitting power laws with  $L$  have exponents 1.63 and 1.69 respectively, however the curve corresponding to a 1.5 power law also provides a reasonable fit to the data. This suggests in these small diameter jets, where capillary thinning is extremely rapid, that the molecular weight dependence arises from increases in the polymer extensibility rather than changes to the relaxation time.

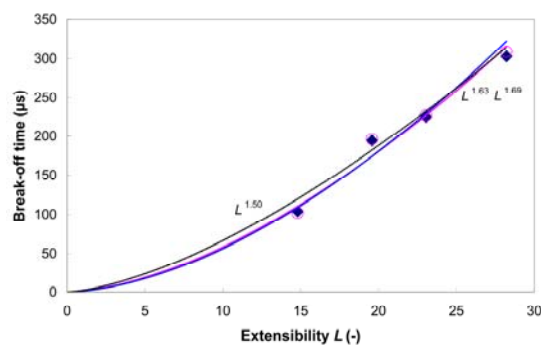


Figure 11 shows the break-off time data at 35 V ( $\blacklozenge$ ) and 32 V ( $\circ$ ) drive voltage with fitted power law curves in extensibility  $L$  together with the  $L^{1.5}$  power law prediction (see text).

Next we consider the final drop speeds, which is plotted in Figure 12 against (a) the Zimm time, and (b) the extensibility  $L$ , for the PS and Newtonian fluids, with trend lines guiding through the data at 35 V (●) and 32 V (○) drive voltages. The Newtonian fluid jetting results are plotted as  $\lambda_z = 0 \mu\text{s}$  in Figure 12(a) and as  $L = 0$  in Figure 12(b).

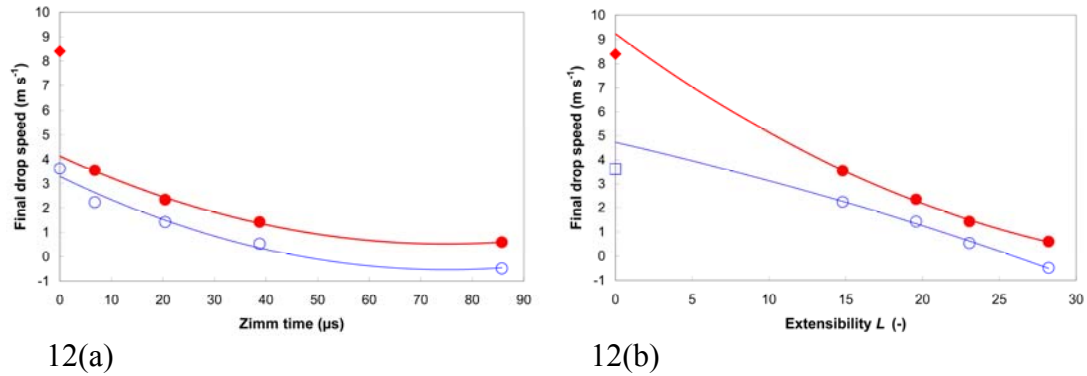


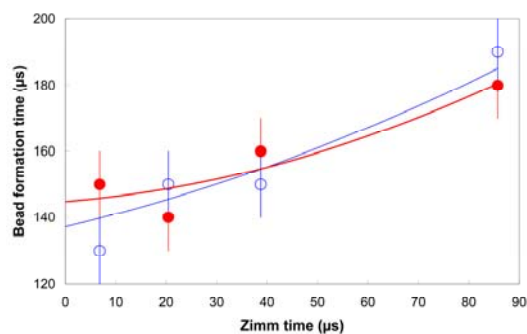
Figure 12 shows the final drop speed at 35 V (●) and 32 V (○) drive voltage as functions of (a) Zimm time and (b) extensibility for the PS solutions. The final Newtonian drop speeds are shown corresponding to 0  $\mu\text{s}$  Zimm time and 0 extensibility. Curved trend lines guide the eye through the PS results for each drive voltage, with the Newtonian drop speed for 35 V (◆) and 32 V (□) drive voltages shown separately. (See text).

The observed final drop speed for the PS solutions is below that of the Newtonian comparison fluid drop, decreasing (through zero speed for 32 V drive voltage) for increasing relaxation time. The Newtonian fluid drop speed for 35 V drive voltage was significantly higher than the trend for the PS solutions extrapolated to the Zimm time of 0  $\mu\text{s}$ . However, as noted for Figure 9(b) above this is a consequence of the early break-up of the leading Newtonian drop from the rest of the trailing ligament in Figure 4(b), marking this speed value as qualitatively different from the final drop speeds for the PS solutions.

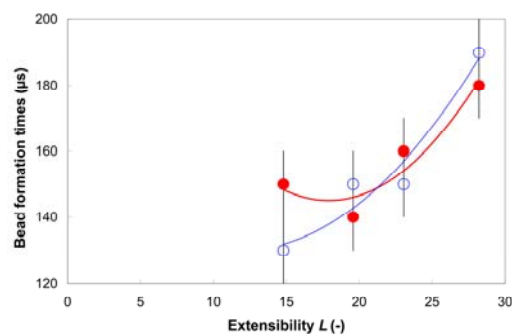
In Hoath, Harlen and Hutchings [3] we presented a simple model for the reduction in head drop speed caused by the viscoelastic stresses in the ligament attaching the drop head to the fluid meniscus in the nozzle. For large Weissenberg numbers there are predicted to be two regimes. When the jet Weissenberg number lies in the range  $1 < Wi < L$ , which is the case for all the solutions considered in this study (when using  $\lambda_z$ , as the relaxation time), the polymers first extend, but subsequently relax as the average extension-rate in the ligament reduces below the inverse relaxation time. In this regime the fractional slowing down (change in drop speed divided by initial speed assumed equal to the Newtonian drop speed in Table II) is proportional to  $G\lambda^2 = \eta_p \lambda$  (where  $\eta_p = \eta - \eta_s$  is the polymer contribution to solution viscosity  $\eta$  above the solvent viscosity  $\eta_s$ ). For these solutions  $G\lambda^2$  increases by a factor of 1.5 from PS210 to PS488, which is roughly consistent with the decrease in speed observed in experiments. However, for larger Weissenberg numbers,  $Wi > L$ , a different regime of behaviour is found, in which the polymers become fully extended. In this regime the fractional slowing down is proportional to  $\eta_p L$ . Although,  $Wi = (U/D)\lambda_z < 0.6L$ , for all the solutions studied here, as recently pointed out by McIlroy *et al* [6], this definition of the regime boundary ignores both the enhancement of extensional

relaxation times above the Zimm time at higher concentrations (see figure 2) and pre-stretching of the polymer molecules within the nozzle, either of which could allow full stretching to take place during the later stages of jetting for higher molecular weight solutions. If this were the case then the reduction in speed would be proportional to  $L$ , as is found in Figure 12(b). Furthermore the gradient is independent of the drive voltage. This latter observation is consistent with drop speeds measurements for DoD jetting reported recently [23] that showed that while the jets have viscosity-dependent drive voltage thresholds the subsequent increase in speed with voltage is approximately independent of viscosity.

Figure 13 shows the beads formation times plotted against (a) the Zimm time, and (b) the extensibility  $L$ , for the PS and Newtonian fluids, with trend lines guiding through the data at 35 V (●) and 32 V (○) drive voltage. While there is a slight increase in the bead formation time with increasing molecular weight, the range of onset times is quite small and the trend with drive voltage is not consistent. Given the inherent difficulty in defining the exact time of bead formation our conclusion is that the bead formation time does not appear to depend strongly on either Zimm time or extensibility.



13(a)



13(b)

Figure 13 shows PS data at 35 V (●) and 32 V (○) drive voltage from Table II for the beads formation time plotted against (a) Zimm time, and (b) the extensibility  $L$  taken from Table I. Quadratic fits to the data are shown to guide the eye.

These beads-on-a-string structures visible in Figures 5-8 arise from the nonlinear stabilization (due to the build-up of high extensional stresses) of the capillary driven instability on a continuous viscoelastic jet (Bousfield *et al* [33]) and have been observed in long time behaviour of polymer liquid bridges [34, 35]. Although the initial Weissenberg number (as the jet leaves the nozzle is large), the effective Weissenberg number decreases with the increase in jet length [6] and falls to below the critical  $Wi = \frac{1}{2}$  well before the onset of bead formation noted in Table II. This is consistent with the observation that in the numerical simulations of McIlroy *et al* [6], the beading instability is only observed once the polymers in the filament have begun to relax. The growth rate of the beads can be estimated from the linear stability theory of Goldin *et al* [28] for the growth of the capillary instabilities on viscoelastic fluid jets, which was shown earlier to predict a time of 67 μs assuming radius  $R = 15$  μm and low shear-rate viscosity of  $\eta_0 = 16$  mPas. However, this assumes the polymers are their initial unstretched configuration, whereas in practice there will be some residual extension of the polymers.

Figures 6-8 for the faster jetted threads also allow the dynamics of beads to be studied as several individual beads can be identified and their positions progressed with time. Motion of smaller beads along the thinning filament tends to allow their merging with the closer of the main drop head or the trailing beads, as is also visible in Figures 6-8. Motion of the smaller beads along threads is further evidence for the importance of inertia [24].

The speeds and extension rates in DoD jetting are far higher than directly accessible by filament stretching and thinning studies published to date. As a consequence the polymer relaxation time is not the key discriminant of viscoelastic behaviour, since the polymers simply deform approximately affinely at high Weissenberg numbers until they reach the limit of extensibility. Thus, as we have shown, it is extensibility rather than the relaxation time that is the main determinant of viscoelastic behaviour. This explains why the extensional relaxation times determined by VMC do not appear to correlate with the jetting behaviour of these fluids, even though relaxation times as low as 30  $\mu\text{s}$  could be measured. Recent approaches to speed up initial filament stretching rates may eliminate extension rate mismatch with DoD jetting [36], however, this will not necessarily resolve the issue in cases where the relaxation time is not the dominant parameter.

## 5. Conclusions

Weakly elastic PS in DEP fluids, having similar (within a factor of 2) low frequency LVE properties but prepared with different mono-disperse molecular weights, require a more complete rheological characterization in relation to their feasibility for use in inkjet printing. In particular, we have demonstrated that the jetting behaviour observed from a 30  $\mu\text{m}$  diameter DoD nozzle does not appear to be consistent with the extensional relaxation times measurements for these fluids obtained in the recent work of Vadillo, Mathues and Clasen. Rather, the predicted slowing of the main drop and delay in break-off are most probably caused by polymer molecules becoming fully stretched in the thinning ligaments producing an enhanced extensional viscosity, whose molecular weight dependence can be predicted from molecular theory.

This conclusion is a consequence of the high jet speeds and small nozzle diameters in combination with the relatively high viscosity solvent and modest molecular weights of the polystyrene, which results in high Weissenberg numbers and moderate values of the extensibility,  $L$  studied here. As discussed in earlier papers [3, 6], other jetting fluid combinations, such as those of de Gans *et al* [4], lie in a different jetting regime where full extension does not occur and relaxation time controls the viscoelastic behaviour. Consequently inkjet fluid assessment methods need to provide a full characterisation including both linear and nonlinear viscoelastic properties. This complexity suggests assessments of inkjet fluids might have to include jetting from sets of DoD print head devices with different sensitivities to all the various VE parameters [37], rather than reliance on testing without jetting. This was not the expected outcome from the present work but does echo the very pragmatic viewpoint expressed as a “map of misery” by Clasen *et al* [38] and may provide a way forward for future R&D strategies towards ink testing.

## **Acknowledgements**

This work was supported by the UK Engineering and Physical Sciences Research Council (EPSRC) through grant number EP/H018913/1 (Innovation in Industrial Inkjet Technology) and a consortium of UK companies, whose permission to publish and support for this work is acknowledged. Malcolm Mackley provided valuable suggestions for testing fluids with similar LVE; Adrian Walker (EPSRC Engineering Instrument Loan Pool) assisted with the Shimadzu HPV-1 high speed camera system and Adept Electronics high power long duration flash lamps used in the present work. The reviewers are thanked for their several helpful suggestions to improve the paper.

## **References**

- [1] J.R. Castrejón-Pita, W.R.S. Baxter, J. Morgan, S. Temple, G.D. Martin, and I.M. Hutchings, Future, opportunities and challenges of inkjet technologies, *Atomization & Sprays* **23**, 541-565 (2013).
- [2] S. D. Hoath, I. M. Hutchings, G. D. Martin, T. R. Tuladhar, M. R. Mackley, and D. Vadillo, Links between ink rheology, drop-on-demand jet formation, and printability, *J. Imaging Sci. Technol.* **53**, 041208 (2009).
- [3] S. D. Hoath, O. G. Harlen, and I. M. Hutchings, Jetting behaviour of polymer solutions in drop-on-demand inkjet printing, *J. Rheol.* **56**, 1109-1127 (2012).
- [4] B. J. de Gans, E. Kazancioglu, W. Meyer, and U. S. Schubert, Inkjet printing polymers and polymer libraries using micropipettes, *Macromol. Rapid Comm.* **25**, 292-296 (2004).
- [5] A. V. Bazilevskii, J. D. Meyer, and A. N. Rozhkov, Dynamics and breakup of pulse microjets of polymeric liquids, *Fluid Dynamics* **40**, 376-392 (2005).
- [6] C. McIlroy, O. G. Harlen, and N. F. Morrison, Modelling the jetting of dilute polymer solutions in drop-on-demand inkjet printing, *J. Non-Newt. Fluid Mech.* **201**, 17-28 (2013).
- [7] K. A-Alamry, K. Nixon, R. Hindley, J. A. Odell, and S. G. Yeates, Flow-Induced Polymer Degradation During Inkjet Printing, *Macromol. Rapid Commun.* **32**, 316-320 (2011).
- [8] D. C. Vadillo, W. Mathues, and C. Clasen, Microsecond relaxation processes in shear and extensional flows of weakly elastic polymer solutions, *Rheol. Acta* **52**, 755-769 (2012).
- [9] P. P. Bhat, S. Appathurai, M. T. Harris, M. Pasquali, G. H. McKinley, and O.A. Basaran, Formation of beads-on-a-string structures during break-up of viscoelastic filaments, *Nature Physics* **6**, 625-631 (2010).

- [10] O. E. Yildirim and O. A. Basaran, Dynamics of formation and dripping of drops of deformation-rate-thinning and -thickening liquids from capillary tubes, *J. Non-Newt. Fluid Mech.* **136**, 17-37 (2006).
- [11] J. Eggers and E. Villermaux, Physics of liquid jets, *Rep. Prog. Phys.* **71** (2008) 36601 (79pp).
- [12] C. Clasen, J. P. Plog, W. M. Kulicke, M. Owens, C. Macosko, L. E. Scriven, M. Verani, and G. H. McKinley, “How dilute are dilute solutions in extensional flows?”, *J. Rheol.* **50**, 849-881 (2006).
- [13] Y. Christanti and L. M. Walker, Surface tension driven jet break up of strain-hardening polymer solutions, *J. Non-Newt. Fluid Mech.* **100**, 9-26 (2001).
- [14] T. R. Tuladhar and M. R. Mackley, Filament stretching rheometry and break-up behaviour of low viscosity polymer solutions and inkjet fluids, *J. Non-Newt. Fluid Mech.* **148**, 97-108 (2008).
- [15] H. Wijshoff, The dynamics of the piezo inkjet print head operation, *Phys. Rep.-Rev. Sec. Phys. Lett.* **491**, 77-177 (2010).
- [16] D. C. Vadillo, T. R. Tuladhar, A. C. Mulji, S. Jung, S. D. Hoath, and M.R. Mackley, Evaluation of ink jet fluids performance using the “Cambridge Trimaster” filament stretch and break-up device, *J. Rheol.* **54**, 261-283 (2010).
- [17] N. F. Morrison and O. G. Harlen, Viscoelasticity in inkjet printing, *Rheol. Acta* **49**, 619-632 (2010).
- [18] J. J. Crassous, R. Regisser, M. Ballauff, and N. Willenbacher, Characterization of the viscoelastic behavior of complex fluids using the piezoelastic axial vibrator, *J. Rheol.* **49**, 851-862 (2005).
- [19] D. C. Vadillo, T. R. Tuladhar, A. Mulji, and M. R. Mackley, The rheological characterisation of linear viscoelasticity for ink jet fluids using Piezo Axial Vibrator (PAV) and Torsion Resonator (TR) rheometers, *J. Rheol.* **54**, 781-795 (2010).
- [20] P. Szabo, G. H. McKinley, and C. Clasen, Constant force extensional rheometry of polymer solutions, *J. Non-Newt. Fluid Mech.* **169-170**, 26-41 (2012).
- [21] H. Yoo and C. Kim, Generation of inkjet droplet of non-Newtonian fluid, *Rheol. Acta* **52**, 313–325 (2013).
- [22] N. Reis, C. Ainsley, and B. Derby, Inkjet delivery of particle suspensions by piezoelectric droplet ejectors, *J. Applied Phys.* **97**, 094903 (2005).
- [23] S. D. Hoath, W.-K. Hsiao, S. Jung, G. D. Martin, I. M. Hutchings, N. F. Morrison, and O. G. Harlen, Drop speeds from drop-on-demand inkjet print heads, *J. Imaging Sci. Technol.* **57**, 010503 (2013).

- [24] C. Clasen, J. Eggers, M. A. Fontelos, J. Li, and G. H. McKinley, The beads-on-string structure of viscoelastic threads, *J. Fluid Mech.* **556**, 283-308 (2006).
- [25] R. Sattler, C. Wagner, and J. Eggers, Blistering pattern and formation of nanofibers in capillary thinning of polymer solutions, *Phys. Rev. Lett.* **100**, 164502 (2008).
- [26] J. R. Castrejón-Pita, S. D. Hoath, A. A. Castrejón-Pita, et al., Time-resolved particle image velocimetry within the nozzle of a drop-on-demand printhead, *J. Imaging Sci. Technol.* **56**, 050401 (2012).
- [27] H. Dong, W.W. Carr, and J.F. Morris, An experimental study of drop-on-demand drop formation, *Phys. Fluids* **18**, 072102 (2006).
- [28] M. Goldin, J. Yerushalmi, R. Pfeffer, and R. Shinnar, Breakup of a laminar capillary jet of a viscoelastic fluid, *J. Fluid Mech.* **38**, 689-711 (1969).
- [29] J. Eggers, Universal Pinching of 3d Axisymmetrical Free-Surface Flow, *Phys. Rev. Lett.* **71**, 3458-3460 (1993).
- [30] L. Campo-Deano and C. Clasen, The slow retraction method (SRM) for the determination of ultra-short relaxation times in capillary breakup extensional rheometry experiments, *J. Non-Newt. Fluid Mech.* **165**, 1688-1699 (2010).
- [31] D. T. Papageorgiou, On the Breakup of Viscous-Liquid Threads, *Phys. Fluids* **7**, 1529-1544 (1995).
- [32] V. M. Entov and E. J. Hinch, Effect of a spectrum of relaxation times on the capillary thinning of a filament of elastic liquid, *J. Non-Newt. Fluid Mech.* **72**, 31-53 (1997).
- [33] D. W. Bousfield, R. Keunings, G. Marrucci, and M. M. Denn, Nonlinear-Analysis of the Surface-Tension Driven Breakup of Viscoelastic Filaments, *J. Non-Newt. Fluid Mech.* **21**, 79-97 (1986).
- [34] H. C. Chang, E. A. Demekhin, and E. Kalaidin, Iterated stretching of viscoelastic jets, *Phys. Fluids* **11**, 1717-1737 (1999).
- [35] M. S. N. Oliveira, R. Yeh, and G. H. McKinley, Iterated stretching, extensional rheology and formation of beads-on-a-string structures in polymer solutions, *J. Non-Newt. Fluid Mech.* **137**, 137-148 (2006).
- [36] M. R. Mackley, S. A. Butler, D. C. Vadillo, T. R. Tuladhar, S. D. Hoath, and S. Huxley, Fast filament stretching, thinning and breakup, Talk at British Society of Rheology Midwinter meeting, Cambridge, UK, December 16<sup>th</sup> (2013), unpublished.
- [37] S. D. Hoath, J. R. Castrejón-Pita, W.-K. Hsiao, S. Jung, G. D. Martin, I. M. Hutchings, T. R. Tuladhar, D. C. Vadillo, S. A. Butler, M. R. Mackley, C.

McIlroy, N. F. Morrison, O. G. Harlen, and H. N. Yow, Jetting of complex fluids, *J. Imaging Sci. Technol.* **57**, (2013).

- [38] C. Clasen, P. M. Phillips, L. Palangetic, and J. Vermant, Dispensing of rheologically complex fluids: The map of misery, *AIChE. Journal* **58**, 3242-3255 (2012).